PNAS

Supporting Information for

PIF4 enhances the expression of *SAUR* genes to promote growth in response to nitrate.

Matías Ezequiel Pereyra, Cecilia Costigliolo Rojas, Anne Jarrell, Austin S. Hovland, Stephen A. Snipes, Punita Nagpal, David Alabadi, Miguel A. Blázquez, Rodrigo A.Gutiérrez, Jason W. Reed, William M. Gray, Jorge José Casal.

Jorge José Casal

Email: casal@ifeva.edu.ar

This PDF file includes:

Supporting Information Text

Extended materials and methods

Generation of CRISPR-Cas9 and high order *saur* mutants. To generate *saur19/21/22/23/24* and *saur19/20/21/22/23/24 #1* mutants we constructed pCGS833 as described previously (1). Briefly, partially complementary primers with the spacer sequences 5'-GGGTTTCTTGCGGTGTACGT-3' and 5'- GGGTTTCTTGCAGTGTACGT-3' were cloned into pMOD_B2515 and pMOD_C2516 respectively. The resulting plasmids and pMOD_A0108, carrying AtEc1.2:Cas9:AtHSP, were cloned into the T-DNA vector pTRANS_210. The two guide sequences target *SAURs 19/20/21/22/23/24*, as well as *SAURs 13/26/27/29*, and mutation abolishes an Rsa I restriction site in each gene. Plants were genotyped by PCR amplifying each of the above *SAUR* genes and digesting the PCR product with Rsa I (see primers in Table S2). We recovered the s*aur19/20/21/22/23/24/61/62/63/64/65/66/67/68/75* mutant among the progeny of a cross between the *saur61/62/63/64/65/66/67/68/75* (2) and *saur19/20/21/22/23/24 #1* mutant. The *saur61/62/63/64/65/66/67/68/75* mutant was also crossed with the *saur26/27/29/73* mutant (3), and the F1 from this cross was crossed with the *saur19/20/21/22/23/24/61/62/63/64/65/66/67/68/75* mutant. The *saur19/20/21/22/23/24/26/27/29/61/62/63/64/65/66/67/68/73/75* mutant was then identified among progeny of this cross. We introduced to the *saur19/20/21/22/23/24/26/27/29/73/61/62/63/64/65/66/67/68/75* mutant a new CRISPR/Cas9 construct in pDGE4 (4) carrying sgRNAs to target additional *SAUR* genes and identified the *saur9/16/19/20/21/22/23/24/26/27/29/61/62/63/64/65/66/67/68/73/75* mutant among the Basta-sensitive progeny. Alleles were identified and genotyped using gel assays to detect allele-specific polymorphisms in PCR products (see primers in Table S2) and by sequencing.

Generation of *pPIF4:PIF4-LUC* and *p35S:PIF4-GFP* in *chl1-5* mutant background. These lines were obtained by genetic cross between both single lines listed in Table S1. The homozygous *chl1-5* mutant was selected from the F2 segregating population by chlorate sensitivity (5) and further confirmed by PCR using the primers listed in Table S2. The lines containing the *pPIF4:PIF4-LUC* or the *p35S:PIF4-GFP* transgenes were identified by the presence of either luciferase activity using a Centro XS^3 LB 960 Berthold microplate luminometer or fluorescence in a confocal microscope.

β-glucuronidase activity. Seedlings of the transgenic lines bearing the β-glucuronidase (GUS) reporter were harvested 3 hours after the beginning of the nitrate treatment, and immediately fixed in cold acetone 90% for at least 20 minutes. After two washes, the fixed seedlings were incubated in X-Gluc buffer [50 mM Na phosphate (pH 7.0), 5 mM EDTA, 0.1% (v/v) Triton X-100, 5 mM $K_4Fe(CN)_6$, 0.5 mM 7 $K_3Fe(CN)_6$ and 1 mg/ml X-Gluc (GBT)] for the time needed in each case and transferred to 70% ethanol. Once chlorophyll was extracted, the seedlings were photographed with a ccd camera attached to an Olympus SZX12 stereoscopic microscope or with a Nikon D5600 camera with an AF-S Micro-Nikkor 60 mm f/2.8 G ED lens.

Fixation for confocal microscopy. When required to keep the timing of sampling, seedlings were immediately fixed before being observed following a previously stated protocol with slight modifications (6–8). Briefly, seedlings were subjected to vacuum in 1% paraformaldehyde in 1X PBS buffer for at least 10 minutes, then washed three times with 50 mM NH4Cl in 1X PBS, three times in PBS 1X and finally diluted to 0.1X.

Luciferase activity. Luciferase activity levels were recorded at different times and were represented as the average counts per 3 seconds in each well. Twelve hours before starting luciferase readings, 20 µL of D-luciferin 0.5 mM was added to each well. For Figure 2J, images

were acquired using an ImageQuant LAS4000 (GE Healthcare) digital imaging system directly from the seedlings growing in the plastic boxes following the general procedure. Twelve hours before starting the measurements 15 µL of D-luciferin 2.5 mM, prepared in 0.005 % Triton X was added to each plant.

Protein blots. We ground samples of seedlings in liquid nitrogen to obtain a fine powder and extracted total protein with 50 µl extraction buffer consisting of 100 mM Tris-HCl, pH 6.8; 5% sodium dodecyl sulphate (SDS); 20% glycerol, 0.02% bromophenol blue, 10% β-mercaptoethanol, 1 mM phenylmethylsulfonyl fluoride (PMSF), 1× protease inhibitor cocktail (Roche) and 80 µM MG132. We heated (5 min, 95°C), centrifuged (5 min, 13,000 rpm) and separated the proteins by electrophoresis on 12% Acrylamide / Bisacrylamide gels. Membranes were washed with 1X Tris-buffered saline (100 mM Tris-HCl and 120 mM NaCl, pH 7.5) containing 0.05% Tween 20 (TBST) and blocked with 5% skim milk in TBST 1.5 h at room temperature, then probed overnight at 4 °C with primary antibodies and for 1 hour with secondary antibody at room temperature. As primary antibodies we used anti-HA (Sigma H6908), anti-GFP (Abcam ab290) or anti-actin (Sigma A0480) at 1:1000, 1:3000 or 1:1500 dilutions in 5% milk respectively. As secondary we used goat anti-rabbit (Invitrogen A24531) or anti-mouse antibodies conjugated with horseradish peroxidase (HRP) at 1:10,000 dilution. We detected the signal by chemiluminescence using SuperSignal West Femto Maximum Sensitivity Substrate (ThermoFisher Scientific, 34095) and films (Hyperfilm ECL Amersham Cytiva).

Statistics. When comparing two nitrate conditions or several nitrogen conditions, we used Student's *t* tests or one-way ANOVA followed by Tukey tests. When comparing the response to nitrate of different genotypes or plants exposed to different light conditions, we used the stepwise model of multiple regression analysis (Infostat) with nitrate, genotype or light condition, and interaction between the two main factors as explanatory variables. When the interaction was significant, we evaluated the effect of nitrate for each genotype or each light condition with Bonferroni post-tests. When the interaction was not significant, we indicate the effect of the main factor nitrate. We identified the genes showing differential expression in response to the nitrate upshift in Col-0 using DESeq2 (9) incorporating Col-0 and *pif4* data and a *q* value (10) of 0.10. Counts per million were made relative to the sum across all treatments for each biological replicate (to correct for experiment effect). For enrichment of GO terms and protein domains was used ThaleMine (11). We identified *SAUR* genes with reduced promotion by the nitrate upshift in the *pif4* mutant by calculating the ratio between the promotion in *pif4* and the promotion in Col-0 for each one of the three replicate transcriptome experiments and comparing this ratio to 1.0 using *t* tests. For these genes, we calculated the correlation between gene expression and hypocotyl growth measured in the same transcriptome experiment.

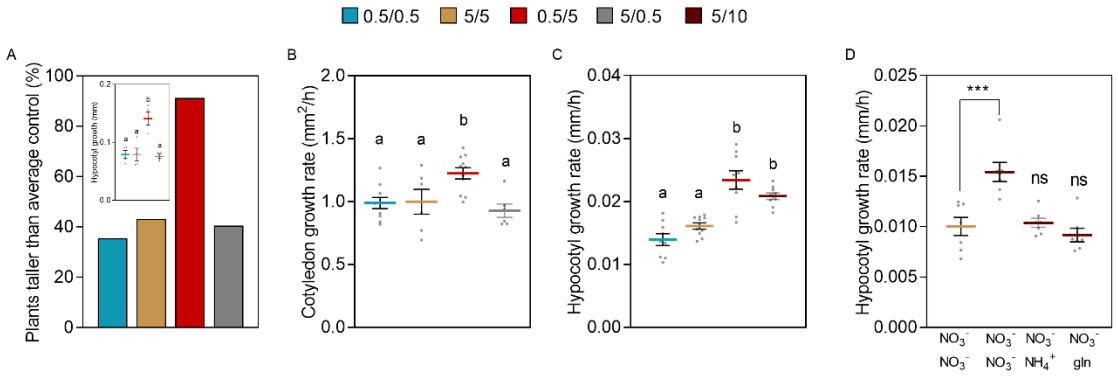

Fig. S1. Growth responds to the increase in nitrate, rather than to the actual dose. (A) Percentage of seedlings taller than an average control seedling grown at 0.5 mM nitrate. The seedlings were grown on 0.5 or 5.0 mM potassium nitrate and either transferred to the contrasting condition or left unchanged, 1 h after the beginning of the photoperiod of day 4. Hypocotyl length was unaffected by the pre-shift condition (0.5 mM: 1.43 ±0.6; 5.0 mM: 1.39 ±0.03, mm). Length increments measured 47 h after the changes in nitrate concentration are shown in the inset. (B) Nitrate upshift promotes cotyledon expansion. Cotyledon expansion rate in seedlings grown on 0.5 or 5.0 mM potassium nitrate and either transferred to the contrasting condition or left unchanged, 1 h after the beginning of the photoperiod of day 4 (growth rates measured between 1 and 10 h after the beginning of the photoperiod). See also Moreno et al. (12), where by day 4, there were no differences in cotyledon expansion between 0.5 and 5.0 mM nitrate). (C) Hypocotyl growth rate in seedlings grown on 0.5- or 5.0-mM potassium nitrate and transferred respectively to the 5.0- or 10.0-mM potassium nitrate 1 h after the beginning of the photoperiod of day 4 (controls left unchanged are included). (D) Hypocotyl growth rate in seedlings transferred from 5.0 to 10.0 mM nitrate or to 5.0 nitrate plus ammonium or glutamine to provide the equivalent amounts of nitrogen as 10.0 mM nitrate. Data are means ±SE and individual values or percentages. Different letters indicate significant differences ($P < 0.05$) in Tukey tests.

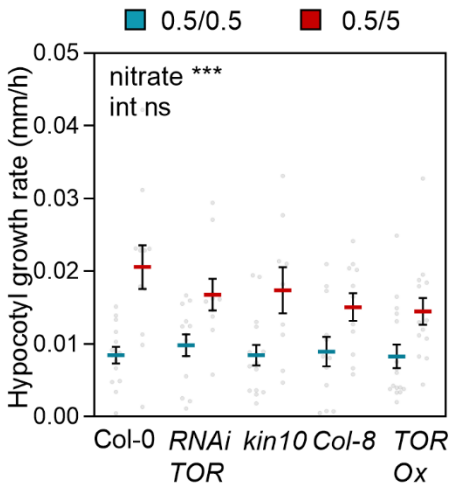

Fig. S2. The TOR pathway does not affect the hypocotyl growth response to a nitrate upshift. Hypocotyl growth rate in seedlings of the wild type (Col-0, Col-8) or affected in the TOR pathway. Seedlings grown on 0.5 mM potassium nitrate and either transferred to the 5.0 mM potassium nitrate or left unchanged, 1 h after the beginning of the photoperiod of day 4. Growth rates measured between 1 and 10 h after the beginning of the photoperiod. Data are means ±SE and individual values. We indicate the significance of the main effect of nitrate from two-way ANOVA that showed no significant genotype by nitrate interaction: ***, $P < 0.001$; ns, not significant.

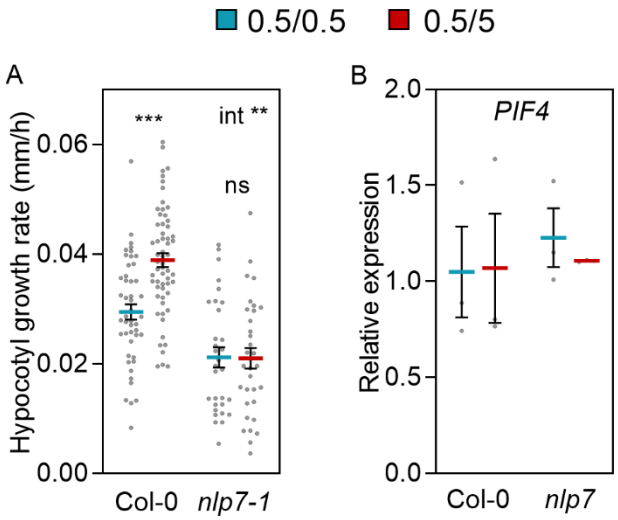

Fig. S3. NLP7 affects hypocotyl growth but not *PIF4* gene expression. (A) Hypocotyl growth in the *nlp7-1* mutant. (B) *PIF4* gene expression in *nlp7-2*. Data are means ±SE and individual values. Asterisks indicate the significance of the effect of nitrate in Bonferroni tests following significant interaction (int): **, P < 0.01; ***, P < 0.001; ns, not significant.

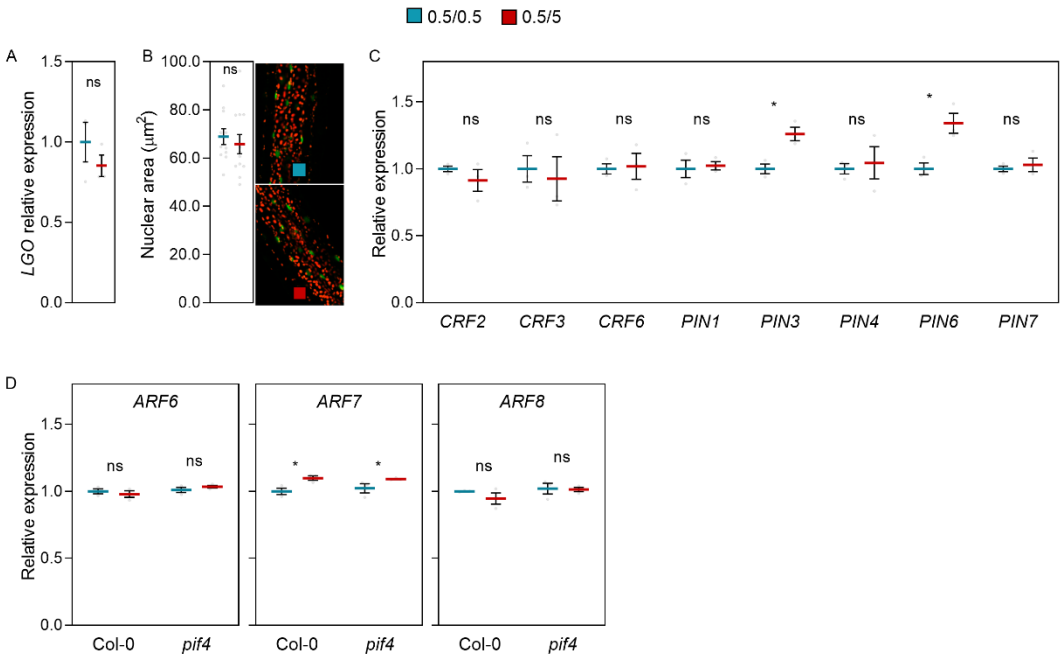

Fig. S4. Analysis of the expression of growth-related genes in response to the nitrate upshift. (A-B) The nitrate upshift did not affect the expression of *LGO* (A) or the size of the nucleus (B, measured in seedlings expressing the *pHY5:HY5-YFP* transgene) in hypocotyl cells. (C), The nitrate upshift did not affect the expression of *CRF2, CRF3, CRF6, PIN1, PIN4* or *PIN7* genes but enhanced the expression of *PIN3* and *PIN6*. (D) The nitrate upshift did not affect the expression of *ARF6* or *ARF8* genes but enhanced the expression of *ARF7*. Seedlings grown on 0.5 mM potassium nitrate and either transferred to the 5.0 mM potassium nitrate or left unchanged, 1 h after the beginning of the photoperiod of day 4. Hypocotyl gene expression from the transcriptome experiment and confocal data recorded 3 h after the nitrate upshift. Data are means ±SE and individual values. We indicate the significance of the effect of nitrate in Student's *t* tests: *, P < 0.05; ns, not significant.

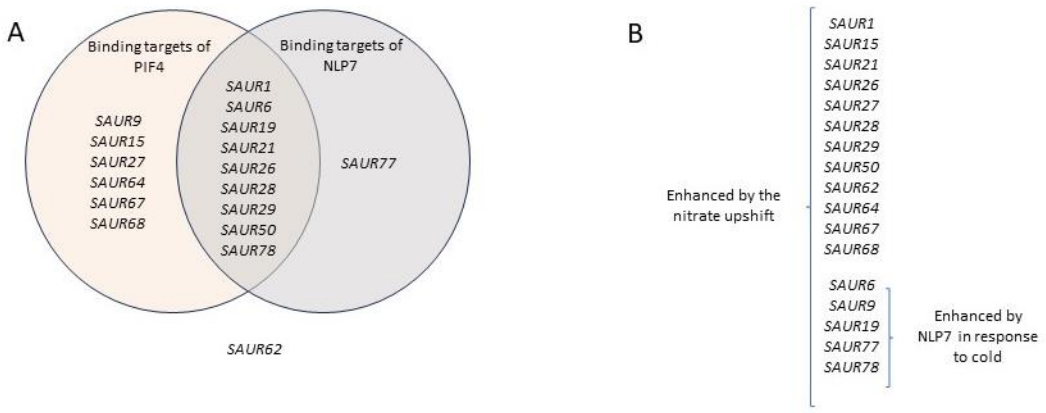

Fig. S5. Most of the *SAUR* genes with expression enhanced by the nitrate upshift are binding targets of PIF4 and/or NLP7. (A) The 17 *SAUR* genes with expression enhanced by the nitrate upshift grouped according to their identification as binding targets of PIF4 (13–15) and/or NLP7 (16–18). (B) Many of the 17 *SAUR* genes with expression enhanced by the nitrate upshift also show NLP7-mediated promotion of expression in response to cold (19).

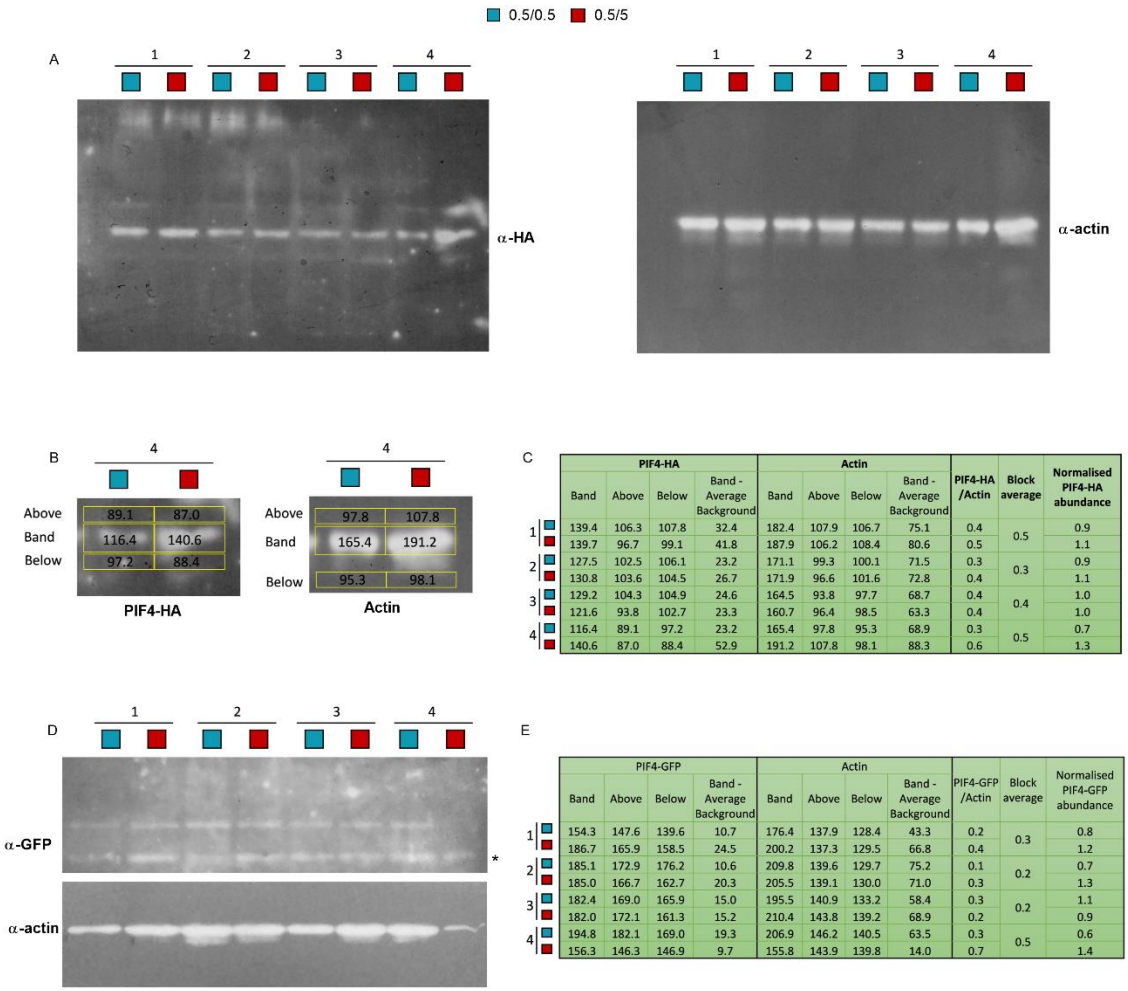

C

	PIF4-HA				Actin				PIF4-HA /Actin	Block average	Normalised PIF4-HA abundance
	Band	Above	Below	Band - Average Background	Band	Above	Below	Band - Average Background			
1	139.4	106.3	107.8	32.4	182.4	107.9	106.7	75.1	0.4	0.5	0.9
	139.7	96.7	99.1	41.8	187.9	106.2	108.4	80.6	0.5		1.1
2	127.5	102.5	106.1	23.2	171.1	99.3	100.1	71.5	0.3	0.3	0.9
	130.8	103.6	104.5	26.7	171.9	96.6	101.6	72.8	0.4		1.1
3	129.2	104.3	104.9	24.6	164.5	93.8	97.7	68.7	0.4	0.4	1.0
	121.6	93.8	102.7	23.3	160.7	96.4	98.5	63.3	0.4		1.0
4	116.4	89.1	97.2	23.2	165.4	97.8	95.3	68.9	0.3	0.5	0.7
	140.6	87.0	88.4	52.9	191.2	107.8	98.1	88.3	0.6		1.3

E

	PIF4-GFP				Actin				PIF4-GFP /Actin	Block average	Normalised PIF4-GFP abundance
	Band	Above	Below	Band - Average Background	Band	Above	Below	Band - Average Background			
1	154.3	147.6	139.6	10.7	176.4	137.9	128.4	43.3	0.2	0.3	0.8
	186.7	165.9	158.5	24.5	200.2	137.3	129.5	66.8	0.4		1.2
2	185.1	172.9	176.2	10.6	209.8	139.6	129.7	75.2	0.1	0.2	0.7
	185.0	166.7	162.7	20.3	205.5	139.1	130.0	71.0	0.3		1.3
3	182.4	169.0	165.9	15.0	195.5	140.9	133.2	58.4	0.3	0.2	1.1
	182.0	172.1	161.3	15.2	210.4	143.8	139.2	68.9	0.2		0.9
4	194.8	182.1	169.0	19.3	206.9	146.2	140.5	63.5	0.3	0.5	0.6
	156.3	146.3	146.9	9.7	155.8	143.9	139.8	14.0	0.7		1.4

Fig. S6. Quantification and normalisation of protein blot data. (A) Negative images of the full blots containing four biological replicates (1-4) corresponding to seedlings bearing the *pPIF4:PIF4-HA* transgene transferred from 0.5 mM to 5.0 mM nitrate 1 h after the beginning of the photoperiod of day 4, compared to the controls that remained on 0.5 mM nitrate. The same blot was revealed with anti PIF4-HA (left) or anti actin (right) antibodies. (B) Example of the procedure used for quantification of the intensity of the bands and the background above and below each band. C, Data corresponding to the intensity of each band and its background and calculation of normalised PIF4-HA abundance shown in Fig. 4. (D-E) As in A and C but for seedlings bearing the *p35S:PIF4-GFP* transgene.

Table S1. List of mutants and transgenic lines used in this study.

A. Mutant and transgenic lines used for hypocotyl growth experiments.

arf6-2 (20)
arf7 (nph4-1) (21)
arf8-2 (22)
arf6-2 arf7 (nph4-1) (23)
arf7 (nph4-1) arf8-3 (23)
arf6-2 arf7(nph4-1) arf8-3 (23)
chl1-9 (24)
chl1-5 (5)
cop1–4 (25)
cry1–304 (26)
D2 WT (27)
D2 m331k (27)
hy5-211 (28)
nlp7-1 (29)
nlp7-2 (30)
NRT1.1^{T101A} (24)
NRT1.1^{T101D} (24)
phyB–9 (31)
pif3-3 (32)
pif4-101 (33)
pif5-3 (33)
pif3-3 pif4-2 (34)
pif4-101 pif5-3 (33)
pif3-3 pif4-1 pif5 -3 (34)
pif4-101 pif5-3 pif7-1 (35)
pif1-1 pif3-3 pif4-2 pif5-3(34)
pifq (34) *gai-td1 rga-28* (36)
rga ∆17 (37)
saur9/16/19/20/21/22/23/24/26/27/29/73/61/62/63/64/65/66/67/68/75 (this report)
saur19/20/21/22/23/24 #1 (this report)
saur19/20/21/22/23/24 #12 (38)
saur19/20/21/22/23/24 #17 (38)
saur19/21/23/24 (this report)
saur19/20/21/22/23/24/26/27/29/73/61/62/63/64/65/66/67/68/75 (this report)
saur19/20/21/22/23/24/61/62/63/64/65/66/67/68/75 (this report)
saur61/62/63/64/65/66/67/68/75 (2)
SAUR19 OX, 35S:STREPII-SAUR19 (39)
SAUR63 OX, 35S:SAUR63-YFP-HA (2)
sav3 (40)
yucq (40)

B. Reporter lines

pDR5:GFP pPIF4:PIF4-GFP (41)
p35S:PIF4-GFP (41)
pPIF4:PIF4-LUC (42)
pPIF4:PIF4-LUC chl1-5 (this report)
pRGA1:RGA1-GFP (43)
pCHL1:CHL1-GUS (44)
pARF6:ARF6-GFP (45)
pARF7:ARF7-VENUS (46)
p35S:DII-VENUS (47)
p35S:PHYB-GFP in Landsberg *erecta* (48)

Table S2. Primers used in this study.

Primer name	Sequence (5' to 3')	Use
Saur9F1	CACCATGGCGATAAAGAAGTCGAAC	genotyping *saur9* mutation (loss of *BstXI* site in PCR product in mutant)
Saur9R1	TTATCTGAACATTGAGATGAGAGAAC	genotyping *saur9* mutation (loss of *BstXI* site in PCR product in mutant)
Saur10F1	CACCATGGCAATAAAGAGATCGAGC	screening for *saur10* mutations (none identified)
Saur10R1	TTATCTAAACATGGAGATAAGAGACCT	screening for *saur10* mutations (none identified)
Saur16F1	CACCATGGCGGTAAAGAGATCTTC	genotyping *saur16* mutation (32 bp deletion in mutant)
Saur16R1	TCATCTGATCATGGATGTTAGAG	genotyping *saur16* mutation (32 bp deletion in mutant)
Saur50F1	CACCATGGCTATAATGAAGAAAACTTCAAA	screening for *saur50* mutations (none identified)
Saur50R1	TCATCGGATCATGGATGTTAG	screening for *saur50* mutations (none identified)
CAS9F1	GATTTGCGAGTCATCCACGC	detecting *Cas9* gene
CAS9R1	TACGCCGGATACATTGACGG	detecting *Cas9* gene
PAT-Basta-1F	CATCGAGACAAGCACGGTCA	detecting Basta resistance gene
PAT-Basta-1R	AAACCCACGTCATGCCAGTT	detecting Basta resistance gene
SAUR9-1-sgRNAOligo1	ATTGGCTATGTGGTCCCAATCTCG	constructing sgRNA shuttle vector
SAUR9-1-sgRNAOligo2	AAACCGAGATTGGGACCACATAGC	constructing sgRNA shuttle vector
SAUR9-2-sgRNAOligo1	ATTGGGTGTTGACCGACGTAGACC	constructing sgRNA shuttle vector
SAUR9-2-sgRNAOligo2	AAACGGTCTACGTCGGTCAACACC	constructing sgRNA shuttle vector
SAUR10-1-sgRNAOligo1	ATTGAGGTCATTTTCCGGTTTACG	constructing sgRNA shuttle vector
SAUR10-1-sgRNAOligo2	AAACCGTAAACCGGAAAATGACCT	constructing sgRNA shuttle vector
SAUR10-2-sgRNAOligo1	ATTGTGACCTTTTGGCACGTCTTG	constructing sgRNA shuttle vector
SAUR10-2-sgRNAOligo2	AAACCAAGACGTGCCAAAAGGTCA	constructing sgRNA shuttle vector
SAUR16-1-sgRNAOligo1	ATTGCAAGAAACAATGCTACGACG	constructing sgRNA shuttle vector
SAUR16-1-sgRNAOligo2	AAACCGTCGTAGCATTGTTTCTTG	constructing sgRNA shuttle vector
SAUR16-2-sgRNAOligo1	ATTGTAAACCGGAAAATGTCCCTT	constructing sgRNA shuttle vector
SAUR16-2-sgRNAOligo2	AAACAAGGGACATTTTCCGGTTTA	constructing sgRNA shuttle vector
SAUR50-1-sgRNAOligo1	ATTGGGACACTTCCCTGTCTATGT	constructing sgRNA shuttle vector
SAUR50-1-sgRNAOligo2	AAACACATAGACAGGGAAGTGTCC	constructing sgRNA shuttle vector
SAUR50-2-sgRNAOligo1	ATTGCCTTTGGTACGTCAAGCGGA	constructing sgRNA shuttle vector
SAUR50-2-sgRNAOligo2	AAACTCCGCTTGACGTACCAAAGG	constructing sgRNA shuttle vector
Saur26F1	CACCATGGCTTTGGTGAGAAGTC	genotyping *saur26/27/29/73* cluster
Saur26R1	TGCTAAGTCGTCAAGTGATATC	genotyping *saur26/27/29/73* cluster
Saur 65 Prom F	CACC CTC AGC CGA AAG ATG GTG AT	genotyping *saur61-saur64* deletion (7728 bp PCR product in wild type, 3.2 kb in mutant)
Saur 61 Gen R	AAA TAC AAG CCG AGT ACT ACT ATG	genotyping *saur61-saur64* deletion (7728 bp PCR product in wild type, 3.2 kb in mutant)
TAL C Saur 64 PR	TTG AGA CCC TTA GGA ACC GTT GA	genotyping *saur61-saur64* deletion (5350 bp PCR product in wild type, 0.8 kb in mutant)
Saur 61 Gen R	AAA TAC AAG CCG AGT ACT ACT ATG	genotyping *saur61-saur64* deletion (5350 bp PCR product in wild type, 0.8 kb in mutant)
Saur 66 PF	CACC CAC AGT TCC ATC TTT GTG TCA	genotyping *saur66* mutation (3402 bp PCR product in wild type, smaller in mutant)
TAL AB 29520 R	CAA TGC CTA GAA CGA TCA CAT A	genotyping *saur66* mutation (3402 bp PCR product in wild type, smaller in mutant)
TS S75-5	ATA TGG TAA GAC GGA TTT GG	genotyping *saur75* deletion (932 bp in wild type, smaller in mutant)
GS S75-3	AGA GAT AAA GAT TTG TAA GC	genotyping *saur75* deletion (932 bp in wild type, smaller in mutant)
Saur19F1	CCAACAACAAGCATTCC	genotyping *saur19* mutation (loss of *RsaI* site in mutant)

Saur19R1	TGTTAGATGTTCCACTTAATTG	genotyping *saur19* mutation (loss of *RsaI* site in mutant)
Saur24F1	ACTCCTTAGTTGATCTTGC	genotyping *saur24* mutation (loss of *RsaI* site in mutant)
Saur24R1	GGATCATCATCATTGGAGC	genotyping *saur24* mutation (loss of *RsaI* site in mutant)
SAUR13F	ATGGGAGTGTTCCGAGGTCTTATG	genotyping
SAUR13R	ccttgtgaattggatCTAATG	genotyping
SAUR19F	gaaggaaaaaatgttggatcatct	genotyping
SAUR19R	cttcaagagcttcataataattcaaactt	genotyping
SAUR20F	taactaggaagaaaaatgttggctca	genotyping
SAUR20R	aacttgaatcttttcatacatcttcag	genotyping
SAUR21F	taagcttcaaaaacctttcgtaca	genotyping
SAUR21R	ccaaatgtcggatcatcatgaTCA	genotyping
SAUR22F	atgaattaagtctatatctaactcgga;	genotyping
SAUR22R	gacaaatagagaattataaATGGCTC	genotyping
SAUR23F	tttcagacaaaagaaATGGCTTTGG	genotyping
SAUR23R	acaaggaaacaactctatctctaact	genotyping
SAUR24F	ctcacataactcactctttcaatcatc	genotyping
SAUR24R	caagaagaaagaggaaaaagggctcatc	genotyping
SAUR26F	tccatacatcttcacaagcttca	genotyping
SAUR26R	catctTCATCCTTGGAGCTGA	genotyping
SAUR27F	ctctaagcttcaaaagatcaagac	genotyping
SAUR27R	ggaatttctatcttcttgatc	genotyping
SAUR29F	gatttcatcgttcattaaacac	genotyping
SAUR29F	caacaagaagcaatccaagaa	genotyping
chl1-5F	TATCCTTCACACACATGCAC	genotyping (For mutant and wild type)(49)
chl1-5R1	AATGCAGTCATGCAGTTTATGCC	genotyping (For mutant identification)(49)
chl1-5R2	AACTCGAAATGCTCGTGTCC	genotyping (For wild type identification)
UBQ10F	AACTTTGGTGGTTTGTGTTTTGG	qPCR
UBQ10R	TCGACTTGTCATTAGAAAGAAAGAGATAA	qPCR
PIF4F	ACTTCTCCTCCCACTTCTTCTCAAC	qPCR
PIF4R	TGGACTTAGGCTTAACCGTCTCTG	qPCR
SAUR21F	TGTGACTTCTCGGCTCCAAT	qPCR
SAUR21R	TGGACCATGATCTCGTGTCT	qPCR
SAUR6F	AAAGCAGAAGAAGAGTTTGGGTTTG	qPCR
SAUR6R	GCTAAGGCGAGAGGCGAGATC	qPCR
SAUR67F	TGGATGGAGATACAGAAAAGGCT	qPCR
SAUR67R	TGTTGAGTACTCTGTTCTTGCTGT	qPCR

SI References

1. T. Čermák, *et al.*, A Multipurpose Toolkit to Enable Advanced Genome Engineering in Plants. *Plant Cell* **29**, 1196–1217 (2017).

2. P. Nagpal, *et al.*, SAUR63 stimulates cell growth at the plasma membrane. *PLOS Genet.* **18**, e1010375 (2022).

3. Z. Wang, *et al.*, Natural variations of growth thermo-responsiveness determined by SAUR26/27/28 proteins in Arabidopsis thaliana. *New Phytol.* **224**, 291–305 (2019).

4. J. Ordon, *et al.*, Generation of chromosomal deletions in dicotyledonous plants employing a user-friendly genome editing toolkit. *Plant J.* **89**, 155–168 (2017).

5. Y.-F. Tsay, J. I. Schroeder, K. A. Feldmann, N. M. Crawford, The Herbicide Sensitivity Gene CM.1 of Arabidopsis Encodes a Nitrate-Inducible Nitrate Transporter. *Cell* **72**, 705–713 (1993).

6. C. Y. Yoo, D. Williams, M. Chen, Quantitative Analysis of Photobodies. *Methods Mol. Biol.* **2026**, 135–141 (2019).

7. C. Y. Yoo, *et al.*, Direct photoresponsive inhibition of a p53-like transcription activation domain in PIF3 by Arabidopsis phytochrome B. *Nat. Commun. 2021 121* **12**, 1–16 (2021).

8. J. Hahm, K. Kim, Y. Qiu, M. Chen, Increasing ambient temperature progressively disassembles Arabidopsis phytochrome B from individual photobodies with distinct thermostabilities. *Nat. Commun. 2020 111* **11**, 1–14 (2020).

9. M. I. Love, W. Huber, S. Anders, Moderated estimation of fold change and dispersion for RNA-seq data with DESeq2. *Genome Biol.* **15**, 1–21 (2014).

10. J. D. Storey, R. Tibshirani, Statistical significance for genomewide studies. *Proc. Natl. Acad. Sci. U. S. A.* **100**, 9440–9445 (2003).

11. A. Pasha, *et al.*, Araport lives: An updated framework for arabidopsis bioinformatics. *Plant Cell* **32**, 2683–2686 (2020).

12. S. Moreno, *et al.*, Nitrate Defines Shoot Size through Compensatory Roles for Endoreplication and Cell Division in Arabidopsis thaliana. *Curr. Biol.* **30**, 1988-2000.e3 (2020).

13. A. Pfeiffer, H. Shi, J. M. Tepperman, Y. Zhang, P. H. Quail, Combinatorial Complexity in a Transcriptionally Centered Signaling Hub in Arabidopsis. *Mol. Plant* **7**, 1598–1618 (2014).

14. U. V. Pedmale, *et al.*, Cryptochromes Interact Directly with PIFs to Control Plant Growth in Limiting Blue Light. *Cell* **164**, 233–245 (2016).

15. E. Oh, *et al.*, Cell elongation is regulated through a central circuit of interacting transcription factors in the Arabidopsis hypocotyl. *Elife* **2014** (2014).

16. R. C. O'Malley, *et al.*, Cistrome and Epicistrome Features Shape the Regulatory DNA Landscape. *Cell* **165**, 1280–1292 (2016).

17. J. M. Alvarez, *et al.*, Transient genome-wide interactions of the master transcription factor NLP7 initiate a rapid nitrogen-response cascade. *Nat. Commun.* **11**, 1–13 (2020).

18. C. Marchive, *et al.*, Nuclear retention of the transcription factor NLP7 orchestrates the early response to nitrate in plants. *Nat. Commun.* **4**, 1–9 (2013).

19. Y. Ding, *et al.*, CPK28-NLP7 module integrates cold-induced Ca2+signal and transcriptional reprogramming in Arabidopsis. *Sci. Adv.* **8** (2022).

20. P. Nagpal, *et al.*, Auxin response factors ARF6 and ARF8 promote jasmonic acid production and flower maturation. *Development* **132**, 4107–4118 (2005).

21. E. Liscum, W. R. Briggs, Mutations of Arabidopsis in Potential Transduction and Response Components of the Phototropic Signaling Pathway. *Plant Physiol.* **112**, 291–296 (1996).

22. Y. Okushima, *et al.*, Functional Genomic Analysis of the AUXIN RESPONSE FACTOR Gene Family Members in Arabidopsis thaliana: Unique and Overlapping Functions of ARF7 and ARF19. *Plant Cell* **17**, 444–463 (2005).

23. J. W. Reed, *et al.*, Three auxin response factors promote hypocotyl elongation1,2[open]. *Plant Physiol.* **178**, 864–875 (2018).

24. C. H. Ho, S. H. Lin, H. C. Hu, Y. F. Tsay, CHL1 Functions as a Nitrate Sensor in Plants. *Cell* **138**, 1184–1194 (2009).

25. T. W. McNellis, *et al.*, Genetic and molecular analysis of an allelic series of cop1 mutants suggests functional roles for the multiple protein domains. *Plant Cell* **6**, 487–500 (1994).

26. T. C. Mockler, H. Guo, H. Yang, H. Duong, C. Lin, Antagonistic actions of Arabidopsis cryptochromes and phytochrome B in the regulation of floral induction. *Development* **126**, 2073–2082 (1999).

27. J. H. Wong, A. K. Spartz, M. Y. Park, M. Du, W. M. Gray, Mutation of a Conserved Motif of PP2C.D Phosphatases Confers SAUR Immunity and Constitutive Activity. *Plant Physiol.* **181**, 353–366 (2019).

28. J. Shin, E. Park, G. Choi, PIF3 regulates anthocyanin biosynthesis in an HY5-dependent manner with both factors directly binding anthocyanin biosynthetic gene promoters in Arabidopsis. *Plant J.* **49**, 981–994 (2007).

29. J. M. Alonso, *et al.*, Genome-wide insertional mutagenesis of Arabidopsis thaliana. *Science (80-.).* **301**, 653–657 (2003).

30. L. Castaings, *et al.*, The nodule inception-like protein 7 modulates nitrate sensing and metabolism in Arabidopsis. *Plant J.* **57**, 426–435 (2009).

31. J. W. Reed, P. Nagpal, D. S. Poole, M. Furuya, J. Chory, Mutations in the gene for the red/far-red light receptor phytochrome B alter cell elongation and physiological responses throughout Arabidopsis development. *Plant Cell* **5**, 147–157 (1993).

32. E. Monte, *et al.*, The phytochrome-interacting transcription factor, PIF3, acts early, selectively, and positively in light-induced chloroplast development. *Proc. Natl. Acad. Sci. U. S. A.* **101**, 16091–16098 (2004).

33. S. Lorrain, T. Allen, P. D. Duek, G. C. Whitelam, C. Fankhauser, Phytochrome-mediated inhibition of shade avoidance involves degradation of growth-promoting bHLH transcription factors. *Plant J.* **53**, 312–323 (2008).

34. P. Leivar, *et al.*, The Arabidopsis phytochrome-interacting factor PIF7, together with PIF3 and PIF4, regulates responses to prolonged red light by modulating phyB levels. *Plant Cell* **20**, 337–352 (2008).

35. M. de Wit, K. Ljung, C. Fankhauser, Contrasting growth responses in lamina and petiole

during neighbor detection depend on differential auxin responsiveness rather than different auxin levels. *New Phytol* **208**, 198–209 (2015).

36. A. R. G. Plackett, *et al.*, DELLA activity is required for successful pollen development in the Columbia ecotype of Arabidopsis. *New Phytol* **201**, 825–836 (2014).

37. A. Dill, H. S. Jung, T. P. Sun, The DELLA motif is essential for gibberellin-induced degradation of RGA. *Proc. Natl. Acad. Sci. U. S. A.* **98**, 14162–14167 (2001).

38. X. Wang, *et al.*, The Asymmetric Expression of SAUR Genes Mediated by ARF7/19 Promotes the Gravitropism and Phototropism of Plant Hypocotyls. *Cell Rep.* **31**, 107529 (2020).

39. A. K. Spartz, *et al.*, The SAUR19 subfamily of SMALL AUXIN UP RNA genes promote cell expansion. *Plant J.* **70**, 978–990 (2012).

40. Y. Tao, *et al.*, Rapid synthesis of auxin via a new tryptophan-dependent pathway is required for shade avoidance in plants. *Cell* **133**, 164 (2008).

41. O. Pucciariello, *et al.*, Rewiring of auxin signaling under persistent shade. 2–7 (2018).

42. G. Murcia, C. Nieto, R. Sellaro, S. Prat, J. J. Casal, Hysteresis in PHYTOCHROME-INTERACTING FACTOR 4 and EARLY-FLOWERING 3 dynamics dominates warm daytime memory in Arabidopsis. *Plant Cell* **34**, 2188–2204 (2022).

43. A. L. Silverstone, *et al.*, Repressing a repressor: gibberellin-induced rapid reduction of the RGA protein in Arabidopsis. *Plant Cell* **13**, 1555–1566 (2001).

44. F.-Q. Guo, R. Wang, M. Chen, N. M. Crawford, The Arabidopsis Dual-Affinity Nitrate Transporter Gene AtNRT1.1 (CHL1) Is Activated and Functions in Nascent Organ Development during Vegetative and Reproductive Growth. *Plant Cell* **13**, 1761 (2001).

45. E. H. Rademacher, *et al.*, A cellular expression map of the Arabidopsis AUXIN RESPONSE FACTOR gene family. *Plant J.* **68**, 597–606 (2011).

46. B. Orosa-Puente, *et al.*, Root branching toward water involves posttranslational modification of transcription factor ARF7. *Science (80-.).* **362**, 1407–1410 (2018).

47. G. Brunoud, *et al.*, A novel sensor to map auxin response and distribution at high spatio-temporal resolution. *Nat. 2012 4827383* **482**, 103–106 (2012).

48. R. Yamaguchi, M. Nakamura, N. Mochizuki, S. A. Kay, A. Nagatani, Light-dependent Translocation of a Phytochrome B-GFP Fusion Protein to the Nucleus in Transgenic Arabidopsis. *J. Cell Biol.* **145**, 437–445 (1999).

49. S. Muños, *et al.*, Transcript profiling in the chl1-5 mutant of arabidopsis reveals a role of the nitrate transporter NRT1.1 in the regulation of another nitrate transporter, NRT2.1 W inside a box sign. *Plant Cell* **16**, 2433–2447 (2004).